Supporting Information

Li et al. 10.1073/pnas.0812843106

SI Materials and Methods

Construction of the Expression Plasmid pET24-*2lnkdsc$_{19}$cfaEB(His)$_6$*. The *cfaB* gene was amplified from the pNTP513 template (8) by PCR using the primer pair (no. 1) listed in Table S5. The DNA fragment for *cfaB* was inserted at the end of *cfaE* in pET24-*lnkdsc$_{19}$cfaE(His)$_6$* (9) by using the QuikChange site-directed mutagenesis kit (Stratagene), creating the intermediate plasmid pET24-*lnkdsc$_{19}$cfaEB(His)$_6$*. The donor strand in the form of "*lnk-dsc$_{19}$*," where *lnk* is DNKQ, was amplified by PCR from the pET24-*lnkdsc$_{19}$cfaE(His)$_6$* using a primer set containing the BamHI and XhoI sites (No. 2, Table S5). Digestion of the pET24-*lnkdsc$_{19}$cfaEB(His)$_6$* and of the lnk-dsc$_{19}$ PCR product with BamHI and XhoI and subsequent ligation resulted in the final construct pE24-*2lnkdsc$_{19}$cfaEB(his)$_6$*. This construct was moved into *Escherichia coli* BL21(DE3) (Invitrogen) for expression.

Construction of Expression Plasmids pET24-*2lnkdsc$_{15}$cfaBB(His)$_6$*, and pET24-*3lnkdsc$_{15}$cfaBBB(His)$_6$*. The *CfaB* gene was amplified by PCR from the *E. coli* strain H10407 (American Type Culture Collection) with the primer set no. 3 listed in Table S5. The reverse primer contains the donor-strand coding sequence "*lnk-dsc$_{15}$*." The *cfaB* fragment was then cloned into pET24a(+) predigested with NdeI and XhoI. Subsequently, the *cfaB* gene was PCR-amplified again with 2 pairs of primers (the NdeI and SacI pair and the SacI and XhoI pair shown as no. 4 and no. 5 in Table S5, respectively), and were cloned into TOPO cloning vector pCRXL-TOPO separately and transformed to OneShot Top10F′ competent cells (Invitrogen). Each *cfaB* fragment was confirmed by DNA sequencing, and the respective plasmids were digested with either NdeI–SacI, or SacI–XhoI. DNA segments were recovered from agarose gel and ligated with pET24a(+). The correct plasmid [pET24-*2lnkdsc$_{15}$cfaB(His)$_6$*] with 2 *cfaB* gene segments in tandem was identified and confirmed by DNA sequencing and was subsequently transformed to BL21(DE3) for expression.

Similarly, the pET24-*3lnkdsc$_{15}$cfaBBB(His)$_6$* was constructed with 3 copies of *cfaB* amplified by using 3 sets of primers (primer sets 6, 7, and 8 in Table S5), which were subsequently cloned to pCRXL-TOPO plasmid and confirmed by DNA sequencing. The 3 *cfaB* genes were released with respective restriction enzymes and ligated to pET24a(+) predigested by NdeI and XhoI to yield pET24-*3lnkdsc$_{15}$cfaBBB(His)$_6$*.

Purification of CfaEB. Cultures of BL21(DE3) bearing the plasmid pET24-*2lnkdsc$_{19}$cfaEB(His)$_6$* were grown at 32 °C in APS Super Broth (Difco) containing 50 μg/mL kanamycin to late log phase and induced with 1 mM IPTG for 3 h. Harvested cell pellets were resuspended in a buffer containing 20 mM sodium phosphate (pH 7.4), 500 mM NaCl, and 50 mM imidazole in a 1:4 (wt/vol) ratio and disrupted by 2 cycles of microfluidization (Model 1109 Apparatus; Microfluidic). The lysate was centrifuged at 17,000 × *g* for 45 min at 4 °C. The supernatant was loaded onto a 5-mL HisTrap FF column (GE Healthcare) equilibrated with the same buffer as above. The protein was eluted with a gradient to 300 mM imidazole over 20 column volumes (CVs); CfaEB fractions were pooled and diluted 10-fold with a buffer consisting of 25 mM Mes (pH 6.0) before loading onto a 5-mL HiTrap SP column (GE Healthcare) preequilibrated in 25 mM Mes (pH 6.0). A gradient to 500 mM NaCl over 20 CVs was used to elute protein from the column. The fractions containing CfaEB were pooled, concentrated with an Amicon Ultra-15 centrifugal filter (Millipore) and applied to a Superdex 75 10/300GL column (GE Healthcare) equilibrated with PBS at pH 6.7. Fractions containing CfaEB were pooled and concentrated to ≈10 mg/mL. The purity of the final pooled sample was determined by densitometry on a SDS/PAGE gel. The identity of the proteins was confirmed by N-terminal sequencing and by Western blotting using anti-dscCfaE antibodies (1:1 × 10^6 dilution) and anti-dscCfaB antibodies (1:1 × 10^6 dilution). Protein concentration was determined by BCA protein assay (Pierce).

Purification of CfaBB and CfaBBB. A 5-L culture was made with Super Broth supplemented with 50 μg/mL kanamycin at 37 °C and induced with 1 mM IPTG. Cell pellets suspended in PBS containing a protease inhibitor mixture were disrupted by using a French press operated at 1,500 psi in 2 passes. Supernatant from centrifugation was applied to Ni-NTA resin and eluted over 20 CVs in a buffer containing 20 mM Tris·HCl (pH 8.0), 0.5 M NaCl and a gradient of imidazole from 10 to 500 mM. The CfaBB fractions were pooled and ammonium sulfate was added to achieve 40% saturation before applying to a Phenyl-Sepharose column (GE Healthcare) preequilibrated with 40% saturated ammonium sulfate in 20 mM Tris·HCl (pH 7.5). Protein was eluted with a gradient of 40% saturation to 0% ammonium sulfate in the same buffer over 20 CVs. Fractions containing CfaBB were pooled and dialyzed against a buffer containing 20 mM Tris·HCl (pH 7.5) with 0.1 M NaCl. Purified CfaBB was further analyzed for monodispersity on a Superdex 200 size-exclusion column (GE Healthcare) in a buffer of 20 mM Tris·HCl (pH 7.5), 0.2 M NaCl. The purification of CfaBBB followed exactly the same procedure as for CfaBB.

Crystallization for CfaEB, CfaBB, and CfaBBB. By following the vapor diffusion procedure (20), protein samples of CfaEB, CfaBB, and CfaBBB were crystallized at 15 °C. Commercial crystallization screen kits (Hampton Research and Molecular Dimensions) were used for robotic screening. After initial conditions were identified, optimizations were carried out manually. The CfaEB crystals were obtained by mixing the protein solution [5 mg/mL in 20 mM Mes (pH 6.0), 0.1 M NaCl] in a 1:1 ratio with a well solution of 11% PEG 8000, 0.1 sodium citrate (pH 4.0), 0.2 M Li_2SO_4. The refined condition for crystallizing CfaBB was to mix the protein [5 mg/mL in 20 mM Tris·HCl (pH 7.5), 0.1 M NaCl] with a well solution of 30% PEG 8000, 0.175 M ammonium sulfate in a 1:1 ratio. The CfaBBB protein [5 mg/mL in 20 mM Tris·HCl (pH 7.5), 0.1 M NaCl] was crystallized by mixing 1:1 with 22% PEG 4000, 0.1 M ammonium sulfate, 0.1 M sodium citrate (pH 3.5), 1% ethylene glycol, 2% PEG 400, 1% isopropyl alcohol, 10 mM $MgCl_2$, 0.3% 1,2,3,-heptanetriol.

X-Ray Diffraction Data Collection, Structure Determination, Model Building, and Refinement. Crystals were tested for diffraction quality and for cryoprotection conditions in house with a Rigaku RU-H3R x-ray generator (Rigaku, MSC) and a MAR345 imaging plate scanner (MarUSA). X-ray diffraction data sets reported in this study were collected at 100 K on either a MAR300 CCD or a MAR225 CCD detector at the SER-CAT beamline of the Advanced Photon Source (APS), Argonne National Laboratory. The raw diffraction images were processed by using the program HKL2000 (10). Crystals of CfaEB display the symmetry of the monoclinic space group $P2_1$. Those for CfaBB and CfaBBB belong to the space groups $P2_12_12$ and $C2$, respectively. Statistics on qualities of diffraction data sets, crystal symmetry, and cell parameters are given in Table S1.

We previously determined the crystal structure of the donor-strand-exchanged CFA/I minor subunit CfaE. As a variation on this approach, we genetically engineered fusion proteins comprising covalently linked, donor-strand-complemented CfaE (adhesin) and CfaB (major pilin) proteins in various combinations. These fusions were each amenable to structural analysis by X-ray crystallography alleviating, in part, the paucity of high-resolution structures available for major pilin subunits from bacterial fimbriae. Because previous characterizations had shown that the CfaB subunits in a mature pilus immediately follow the initiating minor subunit CfaE, our approach for obtaining the structure of CfaB was to extend the dscCfaE in the form of a fusion protein of donor-strand-complemented CfaE and CfaB, designated CfaEB. Purified CfaEB was used to produce crystals that diffracted X-rays to 2.1-Å resolution (Table S1). An additional benefit of the CfaEB fusion was that the crystallographic phase problem could be solved by molecular replacement (MR) using the dscCfaE atomic model as a search template. Subsequent difference Fourier calculation revealed clear electron density for the covalently linked, donor-strand-complemented CfaB, into which a complete atomic model was built. The structure of CfaEB complex was solved by MR using the program Phaser (11) in the CCP4 package (12), and using the dscCfaE model as phasing template (PDB ID 2HB0) (13), which yielded an excellent solution (Z score ≈20) for the CfaE part of the complex and identified 1 CfaEB complex in an asymmetric unit. Difference Fourier maps revealed clear electron density for the presence of major pilin domain CfaB and model building was performed with the graphics programs Coot (14) and O (15). Iterative refinement was done with the program Refmac (16) coupled to manual model rebuilding until the structure refinement converged.

We engineered a plasmid to express a fusion protein consisting of the mature CfaB polypeptide from which the first 13 residues of the N terminus had been removed (N-terminal-deleted CfaB, designated "ntdCfaB") and fused at its C terminus a tetrapeptide linker, followed by a donor-strand-complemented variant of CfaB, to produce the dimeric, covalently linked CfaBB fusion protein (Fig. 1*B*). Crystals of CfaBB diffracted X-rays to 2.3-Å resolution. MR phasing identified 2 CfaBB molecules in a crystallographic asymmetric unit and atomic models were refined successfully (Table S1). The expression plasmid for CfaBBB was similarly constructed. Diffraction data sets for CfaBB and CfaBBB crystals were phased similarly using the CfaB domain from the CfaEB structure as the phasing model. Although MR phasing identified 2 CfaBB complexes per asymmetric unit for CfaBB crystals in the space group $P2_12_12$ (Table S1), 1 molecule of CfaBBB was found per asymmetric unit in the space group $C2$ because the calculated Matthews coefficient (V_m) for CfaBB was 2.6 $Å^3 \cdot Da^{-1}$. The CfaBB structure was also refined successfully with the program Refmac. Statistics for the qualities of the refined models for CfaEB, CfaBB, and CfaBBB are given in Table S1.

Structure Analysis. Structure homologues to CfaB were found with the DALI server (ekhidna.biocenter.helsinki.fi/dali_server). Detailed structure alignments were performed in the program O (15). Calculations for the buried surface between 2 domains were done with the program AREAIMOL (17) in the CCP4 package. The electrostatic potential surface was calculated in the program GRASP (18). The calculation of inertial axes for each pilin domain was done with Molman (19).

Introduction of a CfaB/P13F Point Mutation into the CFA/I Operon and Characterization of Resultant Bacteria. The recombinant *E. coli* strain BL21-SI(pMAM2), which contains the CFA/I bioassembly genes under the control of a salt-inducible T7 promoter, has previously been described (13). A single codon change was introduced to make a switch in CfaB residue 13 [the 13 position referent to residue 1 (Val) of mature CfaB, or what would be P36 referent to the initial Met residue in full-length CfaB] from Pro to Phe by site-directed mutagenesis (QuikChange II, Stratagene). The resulting recombinant strain, BL21-SI(pMAM2-CfaB/P13F), was grown under inducing conditions for analysis by transmission electron microscopy and for determination of its mannose-resistant hemagglutination capacity as described below.

For studies of mannose-resistant hemagglutination (MRHA), BL21-SI(pMAM2), BL21-SI(pMAM2-CfaE/R181A), and BL21-SI(pMAM2-CfaB/P13F) were grown in Luria broth without sodium chloride (LBON) at 30 °C with rotary shaking at 200 rpm, to an OD_{600} of 0.8. Fimbrial expression was induced by addition of 200 mM sodium chloride and continued incubation at 30 °C with a reduction of rotary shaking to 100 rpm). Cultures were harvested at 0, 1, and 3 h after the addition of salt, centrifuged at low *g* force, and resuspended in PBS (pH 7.4) with 0.5% D-mannose to a final bacterial concentration of 10^{10} colony-forming units per mL. The MRHA assay was performed with bovine erythrocytes as described previously (see refs. 4 and 13). MRHA results were determined by visual inspection after 5, 10, 15, and 20 min of rocking on ice.

Sample Preparation, Imaging, and Data Digitization for Transmission EM. BL21-SI(pMAM2) (wild type) and BL21-SI(pMAM2-CfaB/P13F) (P13F mutant) were grown on LB agar without NaCl overnight at 30 °C. They were transferred onto LB agar containing 200 mM NaCl, and induced for 6 h at 30 °C. Bacteria were scraped from plates and diluted with Tris-buffered (pH 7.6) saline to an OD_{600} of ≈1.2. Grids for electron microscopy (EM) were prepared by adsorption of 4–8 μL sample onto glow-discharged carbon-coated grids, washed with 10 mM Tris·HCl (pH 7.6), 0.1 mM EDTA, and negatively stained with 1% uranyl acetate. Images were recorded at 25,000–62,000× magnification on a Philips CM12 or FEI TF20 transmission EM on Kodak SO-163 film, and digitized with a Nikon 9000 scanner at 2,000 or 4,000 dots per inch.

1. Nielsen H, Engelbrecht J, Brunak S, von Heijne G (1997) Identification of prokaryotic and eukaryotic signal peptides and prediction of their cleavage sites. *Protein Eng* 10:1–6.
2. Karjalainen TK, Evans DG, So M, Lee CH (1989) Molecular cloning and nucleotide sequence of the colonization factor antigen I gene of *Escherichia coli*. *Infect Immun* 57:1126–1130.
3. Altboum Z, Levine MM, Galen JE, Barry EM (2003) Genetic characterization and immunogenicity of coli surface antigen 4 from enterotoxigenic *Escherichia coli* when it is expressed in a *Shigella* live-vector strain. *Infect Immun* 71:1352–1360.
4. Anantha RP, et al. (2004) Evolutionary and functional relationships of colonization factor antigen i and other class 5 adhesive fimbriae of enterotoxigenic *Escherichia coli*. *Infect Immun* 72:7190–7201.
5. Perez-Casal J, Swartley JS, Scott JR (1990) Gene encoding the major subunit of CS1 pili of human enterotoxigenic *Escherichia coli*. *Infect Immun* 58:3594–3600.
6. Froehlich BJ, Karakashian A, Sakellaris H, Scott JR (1995) Genes for CS2 pili of enterotoxigenic *Escherichia coli* and their interchangeability with those for CS1 pili. *Infect Immun* 63:4849–4856.
7. Sajjan US, Sun L, Goldstein R, Forstner JF (1995) Cable (cbl) type II pili of cystic fibrosis-associated *Burkholderia* (*Pseudomonas*) *cepacia*: nucleotide sequence of the cblA major subunit pilin gene and novel morphology of the assembled appendage fibers. *J Bacteriol* 177:1030–1038.
8. Hibberd ML, McConnell MM, Willshaw GA, Smith HR, Rowe B (1991) Positive regulation of colonization factor antigen I (CFA/I) production by enterotoxigenic *Escherichia coli* producing the colonization factors CS5, CS6, CS7, CS17, PCFO9, PCFO159:H4 and PCFO166. *J Gen Microbiol* 137:1963–1970.
9. Poole ST, et al. (2007) Donor strand complementation governs intersubunit interaction of fimbriae of the alternate chaperone pathway. *Mol Microbiol* 63:1372–1384.
10. Otwinowski Z, Minor W (1997) Processing of x-ray diffraction data collected in oscillation mode. *Methods Enzymol* 276:307–326.
11. Storoni LC, McCoy AJ, Read RJ (2004) Likelihood-enhanced fast rotation functions. *Acta Crystallogr D* 60:432–438.
12. Ccp (1994) Collaborative Computational Project, Number 4, 1994. The CCP4 suite: programs for protein crystallography. *Acta Crystallographica D* 50:760–763.

13. Li YF, et al. (2007) A receptor-binding site as revealed by the crystal structure of CfaE, the colonization factor antigen I fimbrial adhesin of enterotoxigenic *Escherichia coli*. *J Biol Chem* 282:23970–23980.
14. Emsley P, Cowtan K (2006) Coot: Model-building tools for molecular graphics. *Acta Crystallogr D* 60:2126–2132.
15. Jones TA, Zou JY, Cowan SW (1991) Improved methods for binding protein models in electron density maps and the location of errors in these models. *Acta Crystallogr A* 47:110–119.
16. Murshudov GN, Vagin AA, Dodson EJ (1997) Refinement of macromolecular structures by the maximum-likelihood method. *Acta Crystallogr D* 53:240–255.
17. Lee B, Richards FM (1971) The interpretation of protein structures: Estimation of static accessibility. *J Mol Biol* 55:379–400.
18. Nicholls A, Sharp KA, Honig B (1991) Protein folding and association: Insights from the interfacial and thermodynamic properties of hydrocarbons. *Proteins Struct Funct Genet* 11:281–296.
19. Kleywegt GJ, Zou J-Y, Kjeldgaard M, Jones TA (2001) Model building and computer graphics. *International Tables for Crystallography*, eds Rossmann MG, Arnold E (Kluwer Academic Publishers, Dordrecht, The Netherlands), 1st Ed, Vol F, pp 353–356.
20. McPherson A (1982) Preparation and Analysis of Protein Crystals. (Wiley, New York).

Fig. S1. Sequence alignment of the N-terminal region of known and putative major subunits in the class 5 fimbrial family. The N-terminal sequences shown above the dashed line are for major subunits of known fimbriae, while those below the dashed line are for putative major fimbrial subunits (PFS) from genetically related fimbrial operons derived from genome sequences without supportive experimental proof of expression. Highly conserved residues are in red boldface. The extent of β-strands (and labeling) shown above the alignment by arrowed lines are based on the atomic structure of CfaB. The number to the left of each sequence and above the alignment are referent to the first residue of each mature protein as predicted by SignalP (1), while the parenthetical numbers to the left are referent to the Met start residue. The following abbreviations are used (with GenBank accession numbers shown in parentheses): major subunits CfaB (Ec), from CFA/I fimbriae of enterotoxigenic *E. coli* (P02971) (2); CsaB (Ec), from CS4 fimbriae of ETEC (AAK97135) (3); CsuA (Ec), CsuA1 or CsuA2 from CS14 fimbriae of ETEC (AAQ20105 and AAQ20106) (4); CosA (Ec), from PCFO71 fimbriae of ETEC (AAS89773) (4); CooA (Ec), from CS1 fimbriae of ETEC (AAA23596) (5); CsbA (Ec), from CS17 fimbriae of ETEC (AAS89777) (4); CsdA (Ec), from CS19 fimbriae of ETEC (AAQ19775) (4); CotA (Ec), from CS2 fimbriae of ETEC (CAA87761) (6); CblA (Bc), from Cbl pili of *Burkholderia cepacia* (AAA69516) (7); PFS (Se), from putative ''CS1-like'' fimbriae of *Salmonella enteritidis enterica* serovar Heidelberg genome sequence (ZP_02664970); PFS (Sp), from putative fimbriae of *Serratia proteamaculans* genome sequence (YP_001476454); PFS (Ss), from putative fimbriae of *Shigella sonnei* genome sequence (YP_312062.1); PFS (Sm), from putative fimbriae of *Stenotrophomonas maltophilia* genome sequence (YP_002029631); PFS (Ps), from putative fimbriae of *Pseudomonas syringae* pathovar phaseolicola genome sequence (YP_273059).

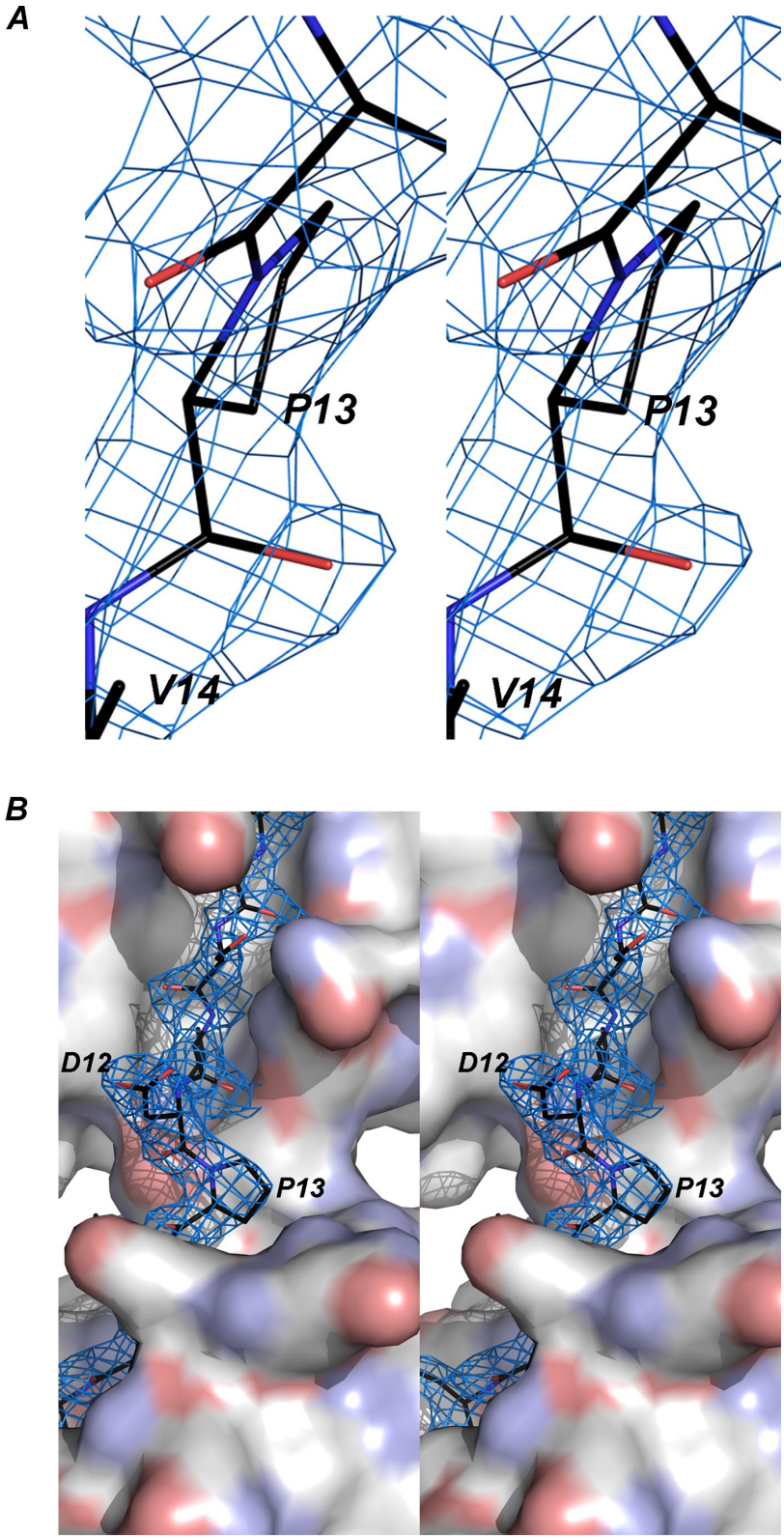

Fig. S2. Structure of CfaBB in the vicinity of Pro^{13}. (*A*) Stereoscopic figure showing the electron density ($2F_o - F_c$) as chicken wire contoured at 1.0 σ for Pro^{13}, which is in the form of sticks with carbon atoms in black, nitrogen blue, and oxygen red. (*B*) Stereo pair showing the molecular surface of CfaBB, focusing on the vicinity of Pro^{13}. The molecular surface is generated in the absence of 11 residues surrounding Pro^{13} with carbon atoms in white, nitrogen in blue, and oxygen in red. The peptide is shown in stick format with carbon in black and is enclosed with chicken wires representing electron density contoured at 1.0 σ.

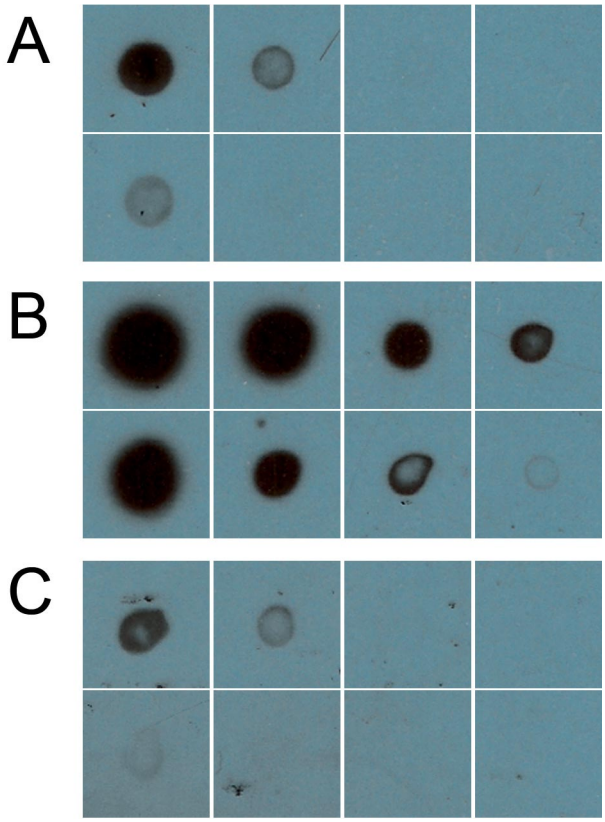

Fig. S3. Dot blot analysis confirms that expressed pilins are localized to the external surface of the bacterium, since antibodies cannot enter the cell. For all blots, 2 μL of bacteria with measured absorbance at 600 nm of 0.4 were dotted onto nitrocellulose paper at (from left to right on each line) full strength or diluted 1/5, 1/25, or 1/250. Upper rows contain bacteria expressing CfaB/P13F. Lower rows contain bacteria expressing wild-type CfaB. After drying, samples were washed with 10mM Tris-HCl, 150mM NaCl, 0.05% Tween20 (pH 8.0); blocked with wash buffer plus 5% non-fat dry milk; incubated in primary antibody overnight at 4 °C; washed; incubated in secondary antibody for 30 min at room temperature; washed again; and visualized with the Pierce Renaissance chemiluminescence kit. All primary antibodies were diluted 1/1000, and secondary antibodies (*A* and *C*, horseradish peroxidase conjugated to goat anti-mouse; *B*, horseradish peroxidase conjugated to goat anti-rabbit) were diluted 1/2000. (*A*) Bacteria labeled with P8D10 monoclonal antibody raised against the adhesin domain of CfaE. (*B*) Bacteria labeled with polyclonal antibodies raised against whole CFA/I fimbriae. (*C*) Bacteria without labeling by primary antibody (control).

Table S1. Statistics on the quality of x-ray diffraction data sets and refinement of structural models

	CfaEB	CfaBB	CfaBBB
Data statistics			
Wavelength, Å	0.7500	1.0000	1.0000
Space group	$P2_1$	$P2_12_12$	$C2$
Cell dimensions, Å	$a = 67.14$	$a = 75.21$	$a = 127.53$
Å	$b = 45.16$	$b = 134.82$	$b = 44.81$
Å	$c = 128.32$	$c = 65.07$	$c = 98.11$
°	$\beta = 97.31$		$\beta = 125.41$
Resolution, Å	2.10	2.25	2.30
No. unique reflections	44,915	32,280	18,583
R_{merge}*†	0.062 (0.229)	0.095 (0.388)	0.057 (0.326)
Completeness,† %	92.0 (75.5)	96.5 (83.4)	91.3 (82.5)
Redundancy†	7.0 (6.1)	5.6 (2.9)	2.9 (2.2)
$\langle I/\sigma_{(I)}\rangle$†	23.0 (7.08)	15.4 (2.4)	11.3 (1.2)
Refinement statistics			
Resolution range, Å	25–2.3	15–2.30	20–2.35
R_{model},† %	0.196 (0.223)	0.247 (0.272)	0.233 (0.302)
R_{free},† %	0.235 (0.255)	0.295 (0.414)	0.287 (0.373)
No. residues	508	608	445
No. protein atoms	3,843	4,371	3,267
No. nonprotein atoms	210	169	82
rmsd bond length, Å	0.019	0.020	0.019
rmsd bond angle, °	1.599	1.965	1.966
Ramachandran plot			
Favored, %	89.5	89.9	92.4
Additional allowed, %	10.3	9.7	7.4
Generously allowed, %	0.2	0.4	0.2
Disallowed, %	0.0	0.0	0.0

*R_{merge} is defined as $\Sigma\,|I_{h,i} - \langle I_h\rangle|/\Sigma I_{h,i}$, where $I_{h,i}$ is the intensity for the ith observation of a reflection with Miller index h, and $\langle I_h[\rangle$ is the mean intensity for all measured values of I_h and their Friedel pairs.

†Numbers in parentheses are for outer-resolution shells.

Table S2. Stability of fusion interfaces as measured by joint and twisting angles between pilin subunits or domains

Subunit	Domains	Joint angle,* °	Twisting angle,† °
CfaE, chain A	CfaEad–CfaEpd	173.5	169.8
CfaE, chain B	CfaEad–CfaEpd	172.8	168.3
CfaEB	CfaEad–CfaEpd	171.6	171.8
CfaEB	CfaEpd–CfaB	138.0	138.4
CfaBB, chain A	CfaB–CfaB	152.2	94.2
CfaBB, chain B	CfaB–CfaB	144.2	112.6
CfaBBB, 1B–2B	CfaB–CfaB	143.8	96.7
CfaBBB, 2B–3B	CfaB–CfaB	145.0	101.6

*Joint angle between 2 domains is defined between longest inertial vectors of each domain.

†Twisting angle between two domains is based on the transformation matrix obtained from structural alignment between domains that share a common interface. The angle represents a rotation in polar space around an axis to bring 2 domains into superposition.

Table S3. Interactions at domain or subunit interfaces

Interface	Buried surface area, Å^2	Hydrogen bonds	Salt bridges
CfaB–CfaB	552	3	0
CfaEad–CfaEpd	700	17	2
CfaEpd–CfaB	505	4	0

Table S4. *E. coli* strains and plasmids used in this work

Strain or plasmid	Description	Reference
E. coli strains		
E. coli H10407	ETEC (CFA/I; LTST; O78:H11)	(1)
TOP10F′	F′[*lacI*^{q} Tn10(tet^{R})] *mcrA* Δ(*mrr-hsdRMS-mcrBC*) ϕ80*lacZ*ΔM15 Δ*lac*X74 *deoR nupG recA1 araD139* Δ(*ara-leu*)7697 *galU galK rpsL*(Str^{R}) *endA1* λ^{-}	Invitrogen
BL21(DE3)	*E. coli* B F^{-} *ompT gal dcm lon hsd*S_B(r_B^{-} m_B^{-}) λ(DE3 [*lacI lac*UV5–T7 gene 1 *ind1 sam7 nin5*])	Novagen
BL21(DE3)pLysS	*E. coli* B F^{-} *ompT gal dcm lon hsd*S_B(r_B^{-} m_B^{-}) λ(DE3 pLysS(cm^{R})	Novagen
Plasmids		
pET24-*lnk2dsc19cfaEB(His)$_6$*	pET24a-based expression plasmid of *cfaE* and *cfaB* with DNKQ linker, dsc19, and C-terminal (His)$_6$ tag	This study
pET24-*lnk2dsc15cfaBB(His)$_6$*	pET24a-based expression plasmid of 2 copies of *cfaB* with DNKQ linker, dsc15, and C-terminal (His)$_6$ tag	This study
pET24-*lnk2dsc15cfaBBB(His)$_6$*	pET24a-based expression plasmid of 3 CfaB copies with DNQK linker, dsc15, and C-terminal (His)$_6$ tag	This study

Table S5. PCR primers used in this work

Primer number	Primer name	Direction	Sequence
1	cfaB	Forward	5′-GTAGAGAAAAATATTACTGTAACAGC
1	cfaB	Reverse	5′-GTGGTGGTGGTGGTGCTCGAGGGATCCCAAAGTCATTACAAGAGA-3′
2	Bdsc19-BamHI	Forward	5′-CGCCGCGGATCCGACAATAAACAAGTAGAGAAAAATATT-3′
2	Bdsc19-XhoI	Reverse	5′-CCGCCGCTCGAGTTGCAAAAGATCAATCACAGGATC-3′
3	cfaB	Forward	5′-ACATATGATTGATCTTTTGCAAGCTGATGGC-3′
3	cfaB	Reverse	5′-CTCGAGAATTGCAGGATCAACACTAGCTGTTACAGTAATATTTTTCTCTACCTGTTTG-TTATCGGATCCCAAAGTCATTACAAGAGATACTAC-3′
4	cfaB-NdeI	Forward	5′-ACATATGATTGATCTTTTGCAAGCTGATGGC-3′
4	cfaB-SacI	Reverse	5′-AGAGCTCAATTGCAGGATCAACACTAGCTGTTA-3′
5	cfaB-SacI	Forward	5′-AGAGCTCTTGCAAGCTGATGGCAATGCTCTGCCA-3′
5	cfaB-XhoI	Reverse	5′-AAGCTTAATTGCAGGATCAACACTAGCTGTTA-3′
6	cfaB-NdeI	Forward	5′-TAACAGCTAGTGTTGATCCTGCAATTTGAaagctt-3′
6	cfaB-SacI	Reverse	5′-aGAGCTCAATTGCAGGATCAACACTAGCTGTTA-3′
7	cfaB-SacI	Forward	5′-aGAGCTCTTGCAAGCTGATGGCAATGCTCTGCCA-3′
7	cfaB-HindIII	Reverse	5′-AAGCTTAATTGCAGGATCAACACTAGCTGTTA-3′
8	cfaB-HindIII	Forward	5′-AAGCTTTTGCAAGCTGATGGCAATGCTCTGCCA-3′
8	cfaB-XhoI	Reverse	5′-CTCGAGAATTGCAGGATCAACACTAGCTGTTACAGTAATATTTTTCTCTACCTGTTTG TTATCGGATCCCAAAGTCATTACAAGAGATACTAC-3′